

## Window-based UFMC technique for 5G systems

Safa N. Idi<sup>1</sup> | Mahmood A. Mahmood<sup>2</sup> | Hasan F. Khazaal<sup>3</sup>

### Affiliations

<sup>1,3</sup> Department of Electrical Engineering, Wasit University, Wasit, Iraq

<sup>2</sup> Ministry of Science and Technology

### Correspondence

Hasan F. Khazaal,  
Department of Electrical Engineering, Wasit University, Wasit, Iraq  
Email:1- [snouri@uowasit.edu.iq](mailto:snouri@uowasit.edu.iq)

3- [hfhahad@uowasit.edu.iq](mailto:hfhahad@uowasit.edu.iq)

### Received

28-February -2021

### Revised

14-March-2021

### Accepted

15-March-2021

Doi: 10.31185/ejuow.Vol9.Iss1.220

### Abstract

In this paper, we investigate the universal filtered multi-carrier system (UFMC) for 5G and subsequent connections with the aid of the MATLAB package. It can be considered that the UFMC technology provides an advantage against inter-symbol interference (ISI) as well as inter-carrier interference (ICI) and low latency. The proposed system is simulated and analyzed in terms of error rates, the complementary cumulative distribution function (CCDF), peak-to-average power ratio (PAPR), error vector magnitude (EVM). In more specific, this paper shows a comparison of two UFMC systems, one with Dolph-Chebyshev filter and the other with Kaiser filter. Obtained results indicate that the performance of the UFMC with Kaiser is quite better than UFMC with Dolph-Chebyshev. Kaiser filter is employed in place of UFMC-based Dolph -Chebyshev to achieve better spectral energy and also to prevent leakage of the spectra. The obtained results also show the enhancement in the EVM and the power spectral density (PSD) criteria, e.g., Kaiser filter enhances the EVM by almost 0.2%. Furthermore, in contrast to applying the Dolph-Chebyshev window in UFMC, the Kaiser window can help in the decrease of PAPR for UFMC.

**Keywords:** 5G; Kaiser filter, Dolph–Chebyshev filter, universal filter multicarrier (UFMC), peak to average power ratio (PAPR), CCDF.

**الخلاصة:** في هذا البحث تم التحري عن استعمال منظومة المرشح العمومي للترددات المتعددة (UFMC) لأغراض خدمات الجيل الخامس من شبكات الاتصال الراديوية، لقد تم انجاز هذا العمل من خلال اجراء عملية محاكاة لشبكة الاتصال لاسلكية تحتوي على هذا النوع من المرشحات (UFMC)، وذلك بالاستفادة من برمجيات (MATLAB). ان تكنولوجيا المرشح العمومي للترددات المتعددة اظهرت فوائد متعددة منها تقليل التداخل بين ترددات الحزمة الفرعية الواحدة (Interference ICI) وكذلك تقليل التداخل بين ترددات الحزم الفرعية المختلفة (ISI Interference) للاشارات اللاسلكية بالإضافة الى ان استخدام هذا النوع من المرشحات (UFMC) يساعد على تقليل التأخير الزمني لتناقل البيانات خلال شبكة الاتصالات. بعد محاكاة الشبكة تم تحليل نتائج محاكاتها من خلال اعتماد بعض المعالم (Parameters) مثل نسبة الخطأ (Error rate) ووظائف الشبكة من خلال التوزيع التراكمي التكميلي (CCDF) والنسبة بين قيمة اعلى قدرة للاشارة الى معدلها (PAPR) بالإضافة الى قيمة متجه الخطأ (EVM). ان محاكاة منظومة المرشح (UFMC) تم بنائها مرتين، الاولى كانت باستعمال المرشح (Dolph-Chebyshev filter) والثانية باستعمال المرشح (Kaiser filter) وكانت نتيجة المحاكاة لنوعي المرشحات، ان اداء منظومة المرشح (UFMC with Kaiser filter) كان افضل من اداء المنظومة (UFMC with Dolph-Chebyshev filter)، اذ ان المرشح نوع (Kaiser) تم استخدامه لتقليل استهلاك الطاقة للاطيف الترددية وكذلك لتجنب التسريب في الطيف الترددي. ان النتائج المستحصلة من المحاكاة اظهرت ان هناك تحسن في قيمة متجه الخطأ (EVM) وكذلك في معيار كثافة قدرة الطيف الترددي (PSD)، حيث كان التحسن في نسبة متجه الخطأ بمقدار (0.2%) وكذلك فان المرشح نوع (Kaiser) قد ساهم بتقليل نسبة اعلى قدرة للاشارة الى معدلها (PAPR) بمقدار (0.05%).

## 1. INTRODUCTION

5G technologies represent a paradigm shift, as it is the first standard that was envisioned with the Internet of Things in mind, as capacity requirements differ in different IoT applications. At the same time, the industry sectors, along with improved mobile broadband applications, are likely to lead the development of 5G in its early stages. Hence, given the diversity of categories of use cases, the 5G infrastructure should be flexible; This is in order to meet various requirements. One way to give this flexibility is to use network segmentation technology, which is a form of network virtualization that allows many of the logic service networks, referred to as "chips", to be supplied through the same basic physical infrastructure. "Slices" are allowed to present various network properties. Although this technology is available in current technologies, it is likely to be a major feature of the fifth generation of wireless networks, as 5G core networks make network segmentation more efficient.

With 5G technology, orthogonality becomes difficult to maintain due to the effects that OFDM waveform is not good in at least for some applications. The researchers work on other 5G waveforms like cyclic prefix OFDM (CP OFDM), Filter bank Multi-carrier (FBMC) and universal filter multi carrier (UFMC). But some applications may not be compatible with OFDM [1]. In 5G technology, the UFMC filter is used as one of the successful alternatives for the OFDM and FBMC, that it combines the specifications of the OFDM and FBMC. So it presents good performance through its higher spectral efficiency, lower out-of-band (OOB) and highly robustness [2]. In the case of UFMC technology [3], the filter is not taken for each subcarrier separately, but a set of frequency subcarriers (sub-band circuits) consisting of a certain number of adjacent subcarrier frequencies. This strategy allows to minimize out-of-band emissions (OOB) in comparison to the old or legacy OFDM technology while symbol length almost the same. This is satisfied due to digital filtering technology, i.e., a window weight level with a shorter length than other technologies. Therefore, the advantage of UFMC technology is introducing fewer delays in data transmission than other technologies [4]. The high spectral efficiency of OFDM technology is ensured by a fairly close arrangement of frequencies of adjacent oscillation subcarriers, which are generated together so that the signals of all subcarriers are orthogonal. This is achieved by using the inverse fast Fourier transform (IFFT) at the transmitter side and the direct fast Fourier transform (FFT) at the receiver side, and both can be quite easily executed using appropriate signal processing methods [5]. Networks of 5G should use simplified synchronization approaches to provide data transmission in the presence of frequency-time distortion with the use of additional digital cyclic prefixes as additional protection against channel delays. Filters in UFMC technologies can eliminate the use of a cyclic prefix technique guard interval and thereby increase their spectral efficiency compared to the legacy OFDM technology. Also, if the additional filtering becomes insufficient to eliminate or decrease the level of subcarriers side lobes in case of a complicated channel environment, then UFMC technologies are more immune to the time shifts and frequency estimation issues compared to OFDM technology. Therefore, UFMC systems do not impose a complex synchronization scheme and passing on extra training signals which is especially important for low-cost devices. The conventional UFMC applies the Dolph-Chebyshev filter for each sub-band. The key benefits are to reduce the attenuation in the main band. Simultaneously, there is abrupt attenuation in the stopband region to avoid OOB emission (limited transition band). However, a great performance can be performed with higher filter orders, i.e., at the price of computational cost. Consequently, a trade-off between the complexity and the performance required to be optimized [6,7]. Several studies have been suggested to cope with the issue of OOB radiations in the presence of the UFMC system. In Ref. [8], authors introduce a transmit-a windowing-based scheme that overcomes OoB radiations by leaving a controlled amount of ICI in the Orthogonal frequency-division multiplexing system. where the transmit-window the approach is utilized to the overall symbols with an extended symbol duration to limit the ISI. In Ref. [9], authors suggest a simplistic spectrum shaping system for Orthogonal frequency-division multiplexing based cognitive radio schemes to improve bandwidth efficiency and spectral compactness. Authors in Ref. [10] employ the Bohman filter just at the lower- and upper-edge subcarriers to decrease the inter-symbol-interference for UFMC Systems in 5G. They observe that employ subcarrier weighting or filtering to the edge subcarriers of the sub bands can improve the scheme at a lower computational cost.

Unlike previous work in Ref. [10], we suggest employing Kaiser window at the transmitter to mitigate the effect of OOB emission and improve the performance of the system. In the current work, we address the PAPR performance in UFMC systems. After that, we compare the performances of two different windows in terms of error vector magnitude (EVM), PAPR, BER, and power spectral density (PSD) in the presence of additive white Gaussian noise (AWGN) channels. Moreover, investigate different order of QAM techniques. The remainder of this manuscript is organized as follows: Section 2 outlines the UFMC system model, while Section 3 introduces the numerical results and discussion, and the conclusions are presented in Section 3. We utilize lower/upper-case boldface letters to indicate column /matrices vector, whereas lower-case letters indicate scalars.

## 2. UPMC SCHEME PRICIPLE

The UPMC native curriculum is based on aggregating sub-carriers into several sub-bands, filtered independently in each sub-band. In general, UPMC is a waveform prepared for 5G technology. The major benefit of choosing UPMC as the primary proposed for wave in fifth-generation technology is that the UPMC scheme doesn't use a periodic prefix to prevent interference between symbols, this will improve the system spectral efficiency and, consequently, reduce spectral resources [11], [12].

### 2.1. System model

The Universal filtered multi-carrier (UPMC) is a new paradigm of multi-carrier modulation technique that specifies the sub-band waveforms, so that the transmitted signal is obtained without an extra cyclic prefix and consequently enhances the spectrum usage. UPMC employs a zero prefix, which is necessary to construct the receiver. Figure 1 shows the UPMC general architecture of the system. [7].

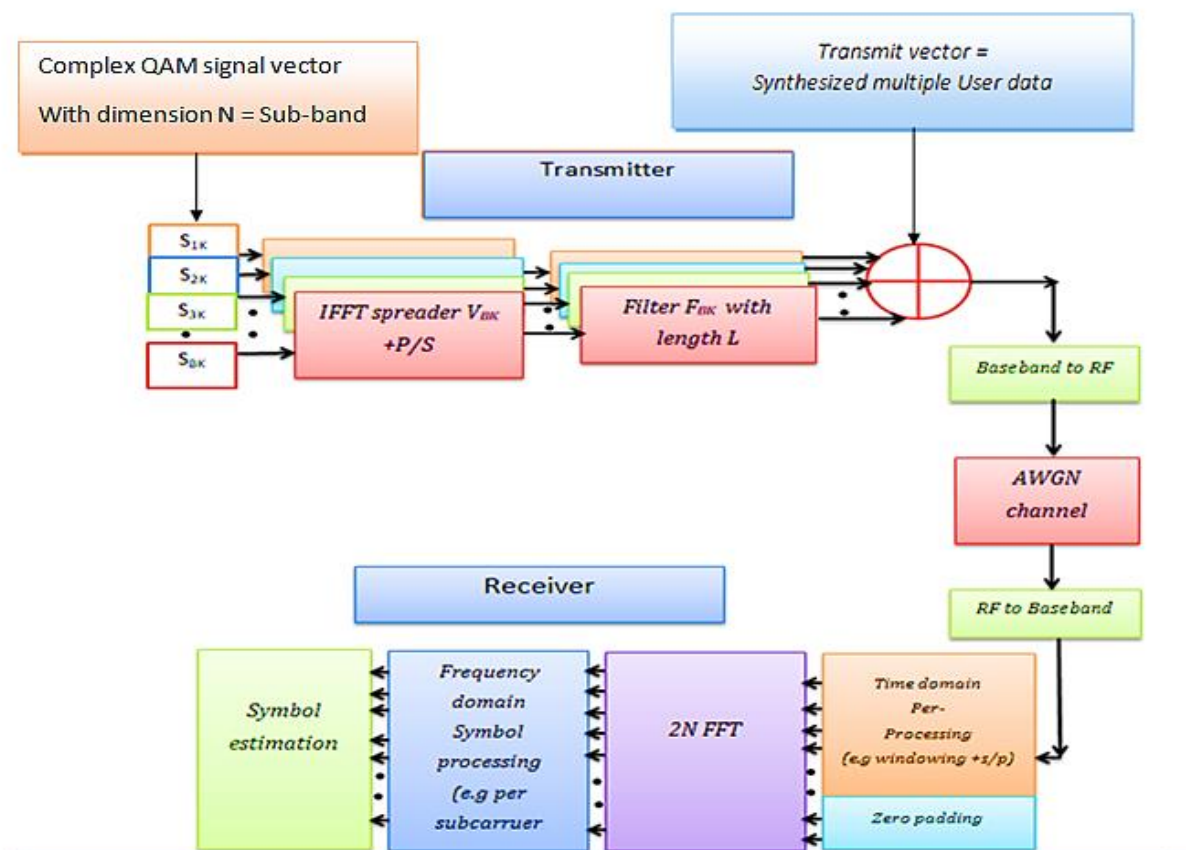


Figure 1: The UPMC system block diagram.

The UPMC system filters the subcarriers instead of the entire band filter as in the OFDM system. Further, the transmit signal in the user's time-domain  $k$  represents the overlap of filtered sub-band waveforms. Multiple carrier adjustments rely on splitting data into multiple parts and sending it across a set of sub-channels so that you can achieve a higher data throughput. The UPMC system is also dependent on (FDM), where input data is divided into sub flows at low rates. [13]. Referring to the figure, the input data is divided into sub-bands. When these sub-bands are utilized, a specific length filter is used for each sub-band, which leads to a significant reduction in out-of-band transmission [1]. In this way, it will reduce bad interference between adjacent sub-channels. UPMC can be achieved using Dolph-Chebyshev Filter and Kaiser Filter. The Kaiser window, also known as the (Kaiser - Bessel window), was developed by James Kaiser at Bell Labs. It is a family of single parameter window functions used in the design of the finite impulse response filter and spectroscopy and increases the energy concentration in the main lobe but is difficult to calculate. Also, Dolph-Chebyshev windows control the breadth of the side lobes with respect to the main lobe, and the correct selection gives good results [1,14]. For the UPMC scheme in figure 1, the transmit signal in the user's time-domain  $k$  represents the overlay of the filtered sub-band waveforms. Assuming that the FFT and filter lengths are, respectively,  $N$  and  $L$ , then the signal delivered by the UPMC can be represented in the matrix and vector shape as given in the following equation [12],

$$X_k = \sum_{i=1}^B F_{i,k} V_{i,k} S_{i,k} \tag{1}$$

Where  $\mathbf{F}_{i,k}$  is the Toeplitz matrix for the sub-beam  $i$ , which contains the pulse responses of the filter leading to the linear fold process and  $\mathbf{V}_{i,k}$  is the IDFT matrix that specifies the nodal codes, and  $S_{i,k}$  is the data beam from the sub-beam request  $i$  after the IFFT is applied with a length of  $N$ .

## 2.2. The Dolph- Chebyshev window

The transformation of the Dolph-Chebyshev window can be expressed in the following equations, [7].

$$W(\mathbf{w}_k) = \frac{\cos\{M \cos^{-1}[\beta \cos(\frac{\pi k}{M})]\}}{\cosh[M \cosh^{-1}(\beta)]}, \quad K = 0,1, \dots, M - 1 \quad (2)$$

Where  $M$  is the length of the window,  $\beta$  and  $\alpha$  are the window parameters, [14].

$$\beta = \cosh\left(\frac{1}{M} \cosh^{-1}(10^\alpha)\right), \quad \alpha \approx 2,3,4, \quad (3)$$

Alpha is a parameter that controls the side-lobe level. Side-lobe level is  $-20 \alpha$  dB. This window can be considered as the ideal Chebyshev lowpass filter impulse response where the main lobe consists of two transition bands (a zero-width pass-band).

## 2.3.Kaiser filter window

The Kaiser window, also known as the (Kaiser - Bessel window), was developed by James Kaiser at Bell Labs. The parameters of the Kaiser window are calculated using the following equation, [14].

$$w(n) = \frac{I_0\left(\beta \sqrt{1 - \left(\frac{n - \frac{N}{2}}{\frac{N}{2}}\right)^2}\right)}{I_0(\beta)}, \quad 0 \leq n \leq N \quad (4)$$

where,  $\beta$  is the coefficient of shape parameter,  $N$  is the length of the filter, and  $I_0(\cdot)$  is the first kind modified Bessel function (zeroth order).

## 2.4. System parameters

The UPMC System will be qualified in two scenarios, the first when using the system with Dolph-Chebyshev filter, while the second is when using Kaiser window. The idea behind these scenarios is to assess the influence of each type of filters on the performance of the system. The general parameters of the system are presenting in table 1. UPMC System parameters: The size and the number of Sub bands are chosen based on the number of FFT points where these values will be chosen for each of the two scenarios that will be compared between them within the UPMC system. The results of the performance comparison of the Kaiser filter and the Dolph-Chebyshev filter will be displayed in next section, in terms of peak-to-average power ratio (PAPR), EVM, and CCDF. Modulation of 64 QAM and 256 QAM will be used for both scenarios.

a. Subband Offset =  $\frac{\text{numFFT}}{2} - \text{subbandSize} * \frac{\text{numSubbands}}{2}$  For band center

b. subbandSize: must be  $> 1$

c. numSubbands \* subbandSize  $\leq$  numFFT

**Table 1:** UPMC design parameters

Parameter	Value
number of FFT points	1024
Sub band Size	50,42
Number of Sub bands	15
Sub band Offset	137
SNR dB	50
Modulation	64QAM , 256 QAM

### 2.4.1 Kaiser window design parameters.

Adjusting the time-bandwidth parameter of the Kaiser window introduces a trade-off balancing between main lobe width and sidelobe amplitude. However, in this type of window, the design process is eliminated to a single parameter optimization problem.

### 2.4.2 Dolph-Chebyshev window design parameters.

The Dolph-Chebyshev window, in contrast to the other type of windows, has two parameters: the shape parameter, and the length of the sequence N. The shape parameter, can be changed with the length of the window is fixed to some points (see table 2). Figure 2 shows Kaiser- filter and Dolph-Chebyshev characteristics in time domain and frequency domain.

Table 2: Dolph-Chebyshev and Kaiser windows design parameters.

Parameter	Value	
	Dolph-Chebyshev	Kaiser
The length of the Filter	30	30
sidelobe attenuation	40	---
Beta	---	5.41

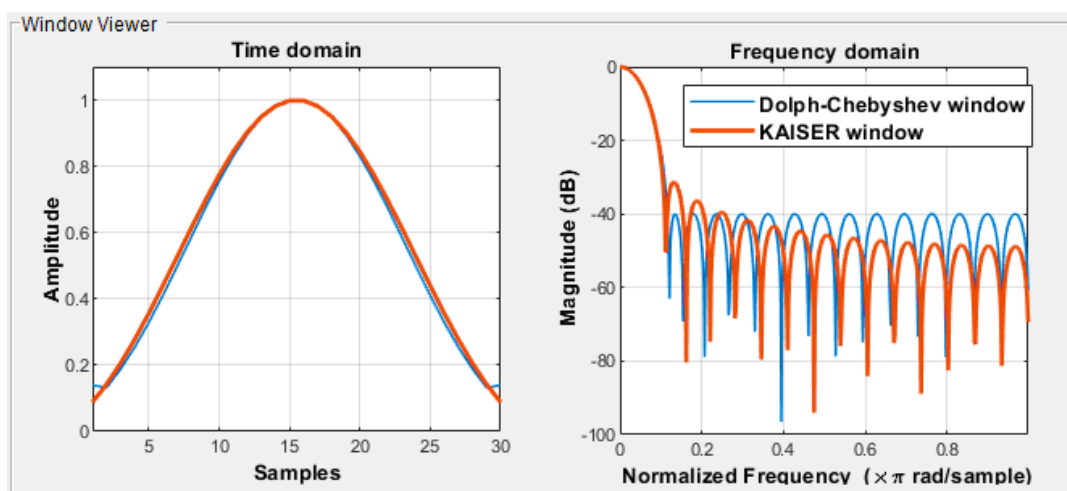


Figure 2: Kaiser- filter and Dolph-Chebyshev characteristics in time domain and frequency domain.

### 2.5. Peak-to-Average Power Ratio (PAPR)

The peak-to-average power ratio (PAPR), is the measure between the highest power and the average power level, and it can be described in the following equation [7,15].

$$PAPR = \frac{|X_{peak}|^2}{x_{rms}^2} \tag{5}$$

Where;  $X_{peak}$  is the highest instantaneous power level and  $X_{rms}$  is the average power level

### 2.6. Error vector magnitude (EVM)

The measured EVM rms measurements using either the average constellation power or the peak constellation power method as Calculated using the following equations [16, 17].

For EVM Normalization method:

The average constellation power:

$$EVM_k = 100 \sqrt{\frac{e_k}{P_{avg}}} \tag{6}$$

$EVM_{rms}$  in percent for average constellation power normalization:

$$EVM_{rms}(\%) = 100 \sqrt{\frac{\frac{1}{N} \sum_{k=1}^N (e_k)}{P_{avg}}} \tag{7}$$

The peak constellation power:

$$EVM_k = 100 \sqrt{\frac{e_k}{P_{max}}} \tag{8}$$

$EVM_{rms}$ , in present for Peak constellation power normalization:

$$EVM_{rms}(\%) = 100 \sqrt{\frac{\frac{1}{N} \sum_{k=1}^N (e_k)}{P_{max}}} \tag{9}$$

$$e_k = (\tilde{I}_k - I_k)^2 + (Q_k - \tilde{Q}_k)^2 \tag{10}$$

Where  $I_k$  and  $Q_k$  represent ideal reference values.  $\tilde{I}_k$  and  $\tilde{Q}_k$  represent measured (received) symbols.

$$EVM(dB) = 20 \log_{10} \left( \frac{EVM_{rms}}{100} \right) \tag{11}$$

## 2.7. Complementary Cumulative Distribution Function (CCDF)

CCDF measurement estimates the CCDF of the random variable  $X$  as defined by the following equation [18, 19] .

$$X = \frac{P}{E(P)} \tag{12}$$

Where

$P$  is the instantaneous power of the signal in watts

$E(p)$  is the mean power of the signal in watts

The following equation defines the CCDF of  $X$ .

$$CCDF_x(X) = pr\{X > x E(P)\} \tag{13}$$

where  $Pr \{e\}$  denotes the probability of the event  $e$ .

## 3. RESULTS AND DISCUSSION

This section explains and displays the results of simulation of the UFMC system in 5G technology with the two pre-defined scenarios, each with candidates filters, and will present the system design results for the filters.

### 3.1. UFMC System Performance for Modulation of 64-QAM

First, we present the spectrum, peak to average power ratio (PAPR), complementary accumulative distribution function (CCDF) for the UFMC system with Kaiser and Dolph-Chebyshev windows.

#### 3.1.1 Effects of Window Length

We investigate a different length for the candidates Dolph-Chebyshev and Kaiser window, where the performance results are scheduled in table 3. According to the obtained results, the length of the candidate window of 30 samples was chosen because it achieved a relatively better result than the rest.

**Table 3:** 64-QAM modulation results for different window length.

Parameter	PAPR		EVM		Average EVM	
	Kaiser	Dolph-Chebyshev	Kaiser	Dolph-Chebyshev	Kaiser	Dolph-Chebyshev
64-QAM modulation <b>Filter length= 20</b>	8.6306 dB	8.6449 dB	0.8 %	0.7 %	-51.4 dB	-51.3 dB
64-QAM modulation <b>Filter length= 30</b>	9.6074 dB	9.6165 dB	0.7 %	0.9 %	-51.2 dB	-51 dB
64-QAM modulation <b>Filter length= 40</b>	10.6377 dB	10.6442 dB	1.2%	1.0 %	-50.5 dB	-50.0 dB
64-QAM modulation <b>Filter length= 50</b>	10.6968 dB	10.6465 dB	1.2 %	2.1 %	-49.0 dB	-47.8 dB

### 3.1.2 End of Transmission Spectral Density

The full sub-band domain is classified into a group of sub-domains. Each sub-band will have a fixed number of sub-carriers where N-pt IFFT will be calculated for each allocated subdomain. Each subdomain is filtered with an L filter, after which these responses are grouped from all different subdomains from each other. The filtering process is used to reduce spectral transmission outside the band path. The same filter will be used for each added subdomain.

The Dolph-Chebyshev window and the Kaiser window with attenuation of side-lobe are used in filtering the IFFT output for each sub-band so that windows are compared and selected the best and most effective. The processing of the end of transmission is shown in Figure 3.

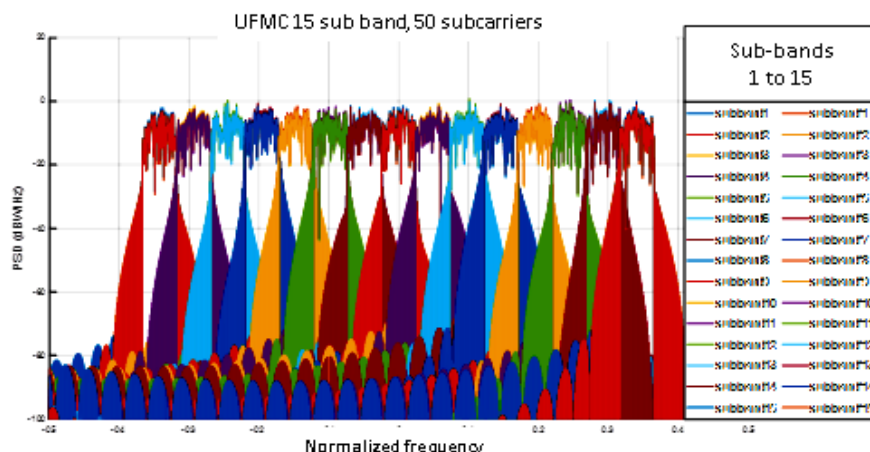


Figure 3: Filtered-UFMC Spectral Density.

### 3.1.3 PAPR Performance

Comparing the UFMC with (Dolph-Chebyshev) and UFMC with (Kaiser) in terms of peak to average power ratio (PAPR) prove that the Kaiser is better according to the following,

1. UFMC with Dolph-Chebyshev: The Peak-to-Average-Power-Ratio is almost 9.6165 dB
2. UFMC with Kaiser: The Peak-to-Average-Power-Ratio is almost 9.6074dB.

### 3.1.4 Rx signal after AWGN 7102 B for UFMC with Kaiser and Dolph-Chebyshev filters

After transmitting the signal to AWGN (SNR is 50 dB), the obtained signal on the reception side is shown in Figure 4. This figure indicates that the UFMC signal with Kaiser filter gives the best signal compared to the Dolph-Chebyshev filter. The maximum magnitude (in dB) received Signal after AWGN-UFMC with Dolph-Chebyshev filter is 31,31 while received Signal after AWGN-UFMC with KAISER filter is 30,27.

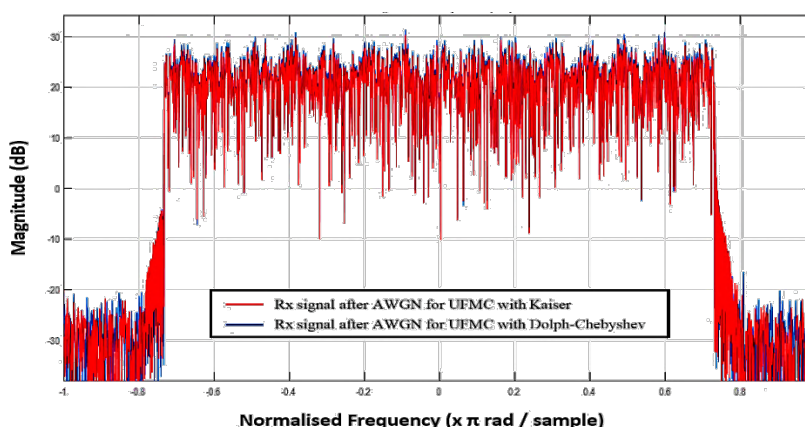


Figure 4: UFMC System  $R_x$  signal after AWGN.



### 3.1.5 Constellation Metric

The error vector magnitude / Modulation error ratio (EVM / MER) [16,17] for the signals of the two systems are compared, and the results show that EVM of the UFMC symbols with Kaiser filter is 0.7 %, and the UFMC symbols equated with Dolph- Chebyshev filter is 0.9 %. Therefore, employing the Kaiser window with the UFMC is better than Dolph-Chebyshev in this aspect.

**Case 1:** UFMC equalized symbols with Dolph-Chebyshev in this scenario, the RMS is 0.3%, Peak EVM is 0.9%, Avg EVM is -51.0 dB, and Peak EVM is -41.3 dB.as shown in the Figure 5.

**Case 2:** UFMC equalized symbols with KAISER filter in this scenario, RMS is 0.3%, Peak EVM is 0.7%, Avg EVM is -51.2 dB, and Peak EVM is -43.1 dB as shown in Figure 6.

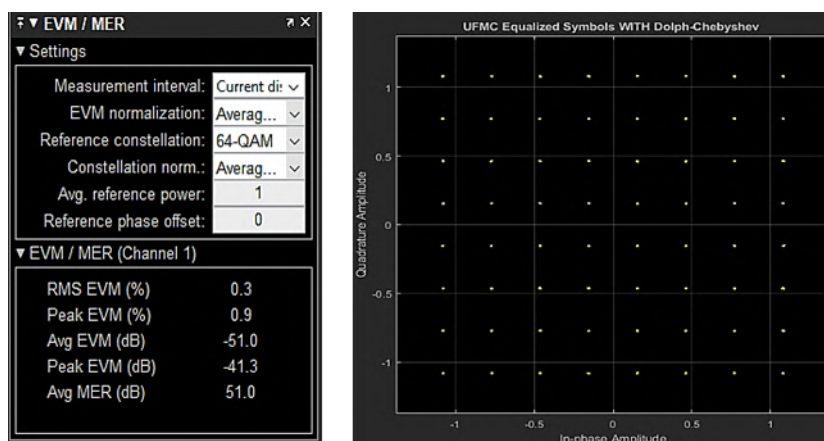


Figure 5: UFMC Equalized Symbols WITH Dolph-Chebyshev.

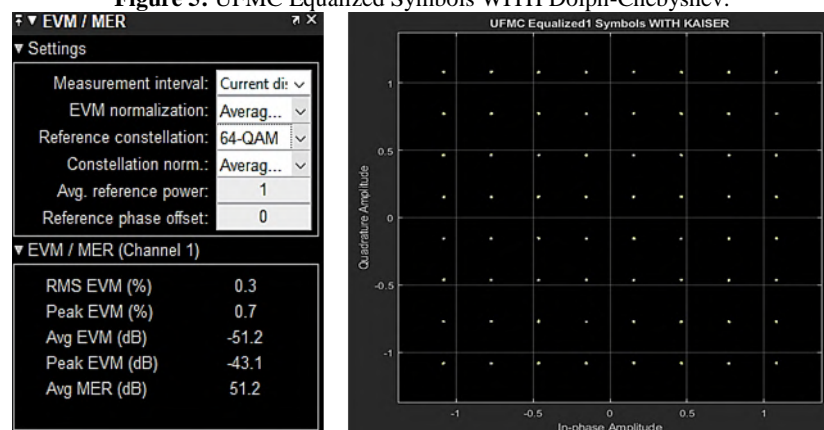


Figure6: UFMC Equalized Symbols WITH Kaiser.

### 3.1.6 Complementary cumulative distribution function (CCDF)

CCDF curves [18] feature high-level power stats for a digitally modified signal. Digitally modified signals are the same amount of time noise as well as frequency. This indicates that statistical signal measurements can be a good description. Also, curves can be good at defining parameters for designing digital communication systems.

**Case 1:** CCDF Measurement for UFMC with Dolph-Chebyshev filter in  $R_x$  signal is shown in Figure 7.



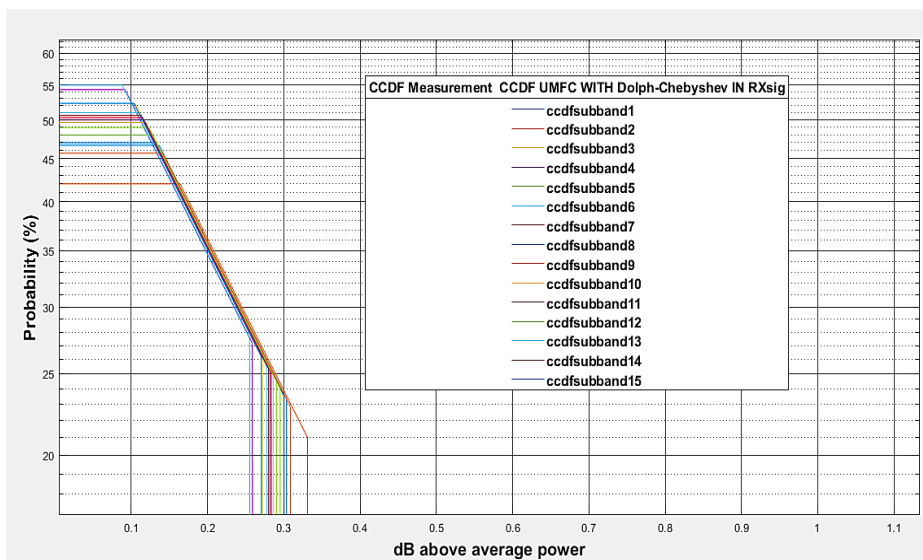


Figure 7: CCDF Measurement CCDF UFMFC with Dolph-Chebyshev filter in  $R_x$  signal.

Case 2: CCDF Measurement for UFMFC with KAISER filter in  $R_{x\text{sig}}$  is shown in Figure 8.

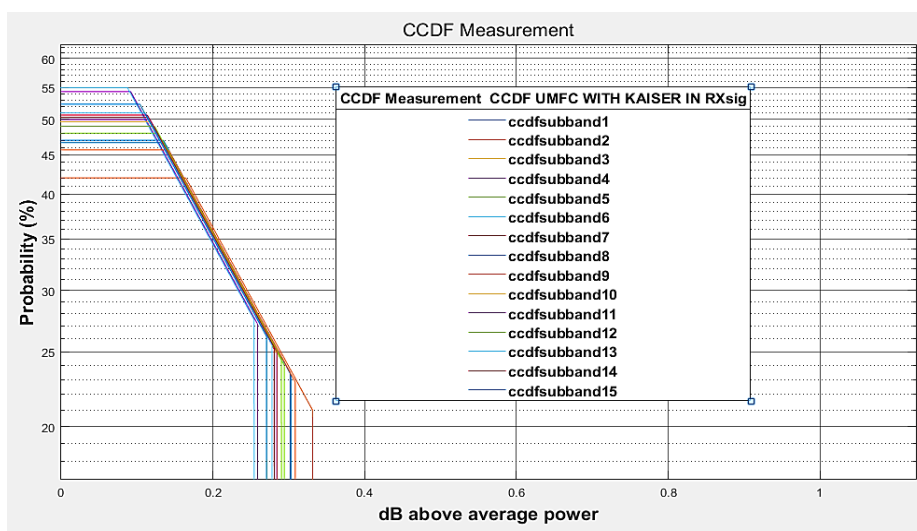


Figure 8: CCDF Measurement CCDF UFMFC with Kaiser filter in  $R_x$  signal.

### 3.2. UFMFC System Performance for Modulation of 256-QAM

Next, we investigate the spectrum, peak to average power ratio (PAPR), complementary accumulative distribution function (CCDF) for the UFMFC system with Kaiser and Dolph-Chebyshev windows for Modulation of 256-QAM. For this case, the Peak-to-Average-Power-Ratio (PAPR) for UFMFC with Dolph-Chebyshev is about 8.1635 dB, while the Peak-to-Average-Power-Ratio (PAPR) for UFMFC with Kaiser is about 8.1107 dB. Also, table 4 summarized the performance of the two filters for two cases of modulation order (64 & 256-QAM) for number of FFT points is 1024 and SNR is 50 dB.

Table 4: UFMFC System Performance Summary

Parameter	64-QAM modulation		256-QAM modulation	
	Kaiser	Dolph-Chebyshev	Kaiser	Dolph-Chebyshev
PAPR	9.6074 dB	9.6165 dB	8.1107 dB	8.1635 dB
EVM	0.7 %	0.9 %	0.6 %	0.7 %
Average EVM	-51.2 dB	-51 dB	-52.1 dB	-52.9 dB

Table 5: Research value compared to previous research on Dolph-Chebyshev in system UFMFC

Parameter	The value of previous research [20] .	Research value
number of FFT points	512	1024
Sub band Size	20	50

Number of Sub bands	10	15
window	Dolph-Chebyshev	Dolph-Chebyshev
SNR dB	15	50
Modulation	16QAM	64QAM
The length of the Filter	43	30
sidelobe attenuation	40	40
PAPR	8.2379 dB	9.6165 dB
EVM	41.7 %	0.9 %

### 3.3. Discussion

We have investigated the performance of the UPMC system of the two scenarios (in the presence of Kaiser filter and Dolph-Chebyshev filter); the results show an improvement in one of the systems which of with Kaiser windows than that with the Dolph-Chebyshev window. The former scheme employs bandwidth much better than the later scheme. The number of sub-bands is 50, and the length of the windows is 30, which is the best in this test. Choosing the best length for the windows will consume the largest possible bandwidth and reduce the error created during the transmission of the signal without affecting the network. Therefore, Kaiser is preferred for the UPMC system in the technology of 5G for better its ability to save data during transmission and reduce data loss when sending it to the receiving side where it shows the EVM percentage of 0.7 while the other is 0.9, i.e., the difference is almost 0.2%.

### 4. CONCLUSIONS

In this study, the performance of the UPMC filtering system is investigated for two scenarios. The system performance with Kaiser type filter is compared with that that employs Dolph-Chebyshev in terms of BER, PAPR, and EVM and PSD and transport effects. Results prove that UPMC with the Kaiser filter gives a key advantage over using Dolph-Chebyshev, and this is why Kaiser filters are applied in the UPMC system rather than other types. This manuscript may introduce an important baseline to get insights about the best signaling design for people investigating 5G wireless schemes and more specific UPMC schemes.

<i>Nomenclatures</i>	
$F_{i,k}$	The Toeplitz matrix for the sub-beam $i$ .
$Io(.)$	The first kind modified Bessel function
$M$	The length of the window
$N$	The length of the filter
Re	Reynolds number
$V_{i,k}$	The IDFT matrix
$S_{i,k}$	The data beam
<i>Greek Symbols</i>	
$\alpha$	a parameter that controls the side-lobe level.
$\beta$	the coefficient of shape parameter.
<i>Abbreviations</i>	
CCDF	Complementary cumulative distribution function
EVM	error vector magnitude
FBMC	Filter bank multicarrier
OFDM	Orthogonal frequency division modulation
OOB	out-of-band emissions
PAPR	peak-to-average power ratio
PSD	Power spectral density
IFFT	the inverse fast Fourier transform
JESTEC	Journal of Engineering Science and Technology
MER	Modulation error ratio
UPMC	universal filtered multi-carrier system

### REFERENCES

[1] Rahman, M. M., Charoenlarnnoppaput, C., Suksompong, P., & Taparugssanagorn, A. (2016). Correlation Coefficient Based DVB-T Continual Pilot Detection to Identify Spectrum Hole for CR Application. Walailak Journal of Science and Technology (WJST), 13(6), 479-490.

- [2] Samad, M. A. (2012). A novel window function yielding suppressed mainlobe width and minimum sidelobe peak. arXiv preprint arXiv:1205.1618.
- [3] Hussain, G. A., & Audah, L. (2020). UFMC system performance improvement using RS codes for 5G communication system. *Telkomnika*, 18(4), 1843-1848.
- [4] Saad, M., Al-Ghouwayel, A., & Hijazi, H. (2018, June). UFMC transceiver complexity reduction. In 2018 25th International Conference on Telecommunications (ICT) (pp. 295-301). IEEE.
- [5] Abou Yassin, M. R., Abdallah, H., Issa, H., & Abou Chahine, S. (2019). Universal Filtered Multi-Carrier Peak to Average Power Ratio Reduction. *Journal of Communications*, 14(3).
- [6] Hu, K. C., & Armada, A. G. (2016, September). SINR analysis of OFDM and f-OFDM for machine type communications. In 2016 IEEE 27th Annual International Symposium on Personal, Indoor, and Mobile Radio Communications (PIMRC) (pp. 1-6). IEEE.
- [7] Cheng, X., He, Y., Ge, B., & He, C. (2016, May). A filtered OFDM using FIR filter based on window function method. In 2016 IEEE 83rd Vehicular Technology Conference (VTC Spring) (pp. 1-5). IEEE.
- [8] Yu, L., Rao, B. D., Milstein, L. B., & Proakis, J. G. (2010, June). Reducing out-of-band radiation of OFDM-based cognitive radios. In 2010 IEEE 11th International Workshop on Signal Processing Advances in Wireless Communications (SPAWC) (pp. 1-5). IEEE.
- [9] Zhou, X., Li, G. Y., & Sun, G. (2012). Low-complexity spectrum shaping for OFDM-based cognitive radio systems. *IEEE Signal Processing Letters*, 19(10), 667-670.
- [10] Mukherjee, M., Shu, L., Kumar, V., Kumar, P., & Matam, R. (2015, August). Reduced out-of-band radiation-based filter optimization for UFMC systems in 5G. In 2015 international wireless communications and mobile computing conference (IWCMC) (pp. 1150-1155). IEEE.
- [11] Wen, J., Hua, J., Lu, W., Zhang, Y., & Wang, D. (2018). Design of waveform shaping filter in the UFMC system. *IEEE Access*, 6, 32300-32309.
- [12] Guo, Z., Liu, Q., Zhang, W., & Wang, S. (2020). Low complexity implementation of universal filtered multi-carrier transmitter. *IEEE Access*, 8, 24799-24807.
- [13] Acquah, S., Krampah-Nkoom, A., & Adjei, M. O. (2020). Performance of the Candidate Modulation Wave-forms for 5G Communication Systems.
- [14] Bergen, S. W., & Antoniou, A. (2005). Design of nonrecursive digital filters using the ultraspherical window function. *EURASIP Journal on Advances in Signal Processing*, 2005(12), 1-13.
- [15] Baig, I., & Jeoti, V. A. R. U. N. (2011). On the PAPR reduction in OFDM systems: a novel ZCT precoding based SLM technique. *Journal of Engineering Science and Technology*, 6(3), 357-368.
- [16] Arbi, T., Nasr, I., & Geller, B. (2020). Near Capacity RCQD Constellations for PAPR Reduction of OFDM Systems. In ICASSP 2020-2020 IEEE International Conference on Acoustics, Speech and Signal Processing (ICASSP) (pp. 5110-5114). IEEE.
- [17] Azarnia, G., Sharifi, A. A., & Emami, H. (2020). Compressive sensing based PAPR reduction in OFDM systems: Modified orthogonal matching pursuit approach. *ICT Express*, 6(4), 368-371.
- [18] Bendimerad, M. Y. (2015). Statistical Peak to Average Power Ratio Bound. *Communication Antenna Propagation*. 5(4): 190-196.
- [19] Acquah, S., Krampah-Nkoom, A., & Adjei, M. O. (2020) Performance of the Candidate Modulation Wave-forms for 5G Communication Systems. 10(6):579-644.
- [20] S. Acquah, A. Krampah-nkoom, and M. O. Adjei, "Performance of the Candidate Modulation Wave - forms for 5G Communication Systems," vol. 10, no. 6, pp. 597-644, 2020, doi: 10.29322/IJSRP.10.06.2020.p10274.